

See discussions, stats, and author profiles for this publication at: <https://www.researchgate.net/publication/319940759>

Tactile-based Object Center of Mass Exploration and Discrimination

Conference Paper · September 2017

CITATION

1

READS

25

3 authors, including:



Kunpeng Yao

Technische Universität München

4 PUBLICATIONS 6 CITATIONS

[SEE PROFILE](#)



Mohsen Kaboli

Technische Universität München

30 PUBLICATIONS 145 CITATIONS

[SEE PROFILE](#)

Some of the authors of this publication are also working on these related projects:



Project

SELFCEPTION: Self/other distinction for interaction under uncertainty [View project](#)



Project

Mask-bot [View project](#)

Tactile-based Object Center of Mass Exploration and Discrimination

Kunpeng Yao, Mohsen Kaboli*, and Gordon Cheng

Abstract—In robotic tasks, object recognition and discrimination can be realized according to their physical properties, such as color, shape, stiffness, and surface textures. However, these external properties may fail if they are similar or even identical. In this case, internal properties of the objects can be considered, for example, the center of mass. Center of mass is an important inherent physical property of objects; however, due to the difficulties in its determination, it has never been applied in object discrimination tasks. In this work, we present a tactile-based approach to explore the center of mass of rigid objects and apply it in robotic object discrimination tasks. This work comprises three aspects: (a) continuous estimation of the target object’s geometric information, (b) exploration of the center of mass, and (c) object discrimination based on the center of mass features. Experimental results show that by following our proposed approach, the center of mass of experimental objects can be accurately estimated, and objects of identical external properties but different mass distributions can be successfully discriminated. Our approach is also robust against the textural properties and stiffness of experimental objects.

I. INTRODUCTION AND RELATED WORK

Tactile object recognition are of great significance in robots’ interaction with the environment [1]. Objects can usually be distinguished from their physical properties such as shape, surface texture, and stiffness [2]–[6]. However, if the target objects have the identical external physical properties, the above-mentioned features can not be applied for discrimination tasks. To declare if the target objects are identical, the robot should also verify their internal properties. Center of mass (CoM) is an important inherent physical property of the objects. It reveals the object’s mass distribution. In particular, CoM is a constant position with respect to rigid objects. However, CoM has never been used in robotic object recognition/discrimination tasks, due to the complexity and difficulty in its determination.

A. Related Work

Several previous work has been done on the topic of estimating the target object’s center of mass. One approach is to estimate the CoM of the target object via robotic manipulation tasks. Atkeson et al. [7], [8] estimated the CoM of the load of a robotic arm during a manipulation task. The CoM position is formulated as a parameter of this robotic-load system and estimated by solving the dynamic equation during manipulation. However, this approach requires accurate models and parameters of the robotic system, and

Kunpeng Yao, Mohsen Kaboli, and Gordon Cheng are with the Institute for Cognitive Systems, Department of Electrical and Computer Engineering, Technical University of Munich, Germany. * Mohsen Kaboli is the corresponding author. Email: mohsen.kaboli@tum.de. Video to this paper: <http://web.ics.ei.tum.de/~mohsen/videos/Humanoids2017.mp4>

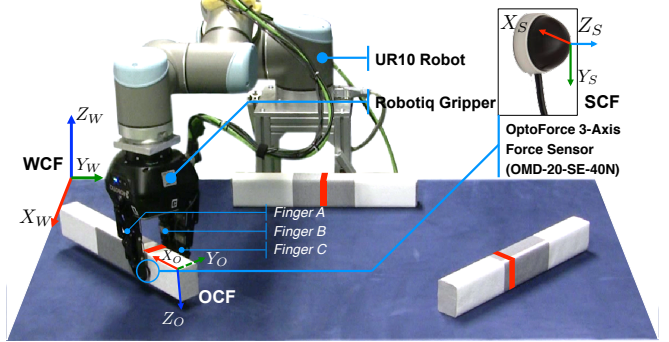


Fig. 1: System description: the UR10 robotic arm, the Robotiq gripper, and the OptoForce 3D Force sensors.

the experimental result was inaccurate due to the unmodeled dynamics. This approach also suffers from the influence of the gravitational torque. Another approach estimate the CoM by executing tipping actions on the object. In [9]–[11], the CoM of the target object is obtained by determining the “gravity equi-effect planes” or the “passing-C.M lines”. The robotic arm installed with force sensors tips the object using its fingertip. The planes or lines that pass through the CoM can be calculated based on the finger position and force information recorded during the tipping movement. However, this approach requires the estimation of the fingertip vector and the accurate representation of lines and planes, which are of high computational complexity. The precise shape, position, orientation of the target object is already given as prior knowledge. In addition, the target object must maintain a stable contact on the table surface without any slip while it is being tilted by the fingertip. In this work, we propose a purely tactile-based approach to determine the CoM of target object, which is model-free and of low computational complexity, thus can be applied in on-line robotic tasks.

B. Contribution

We propose a tactile-based approach to explore the CoM of rigid object in an unknown workspace and apply the CoM feature in robotic object discrimination task.

- We first propose a strategy to continuously estimate the geometric information of regular shaped target objects in an unknown workspace.
- Then, we present a tactile-based approach to explore the CoM of rigid objects by applying lifting actions in a three-sensing-point case.
- Furthermore, we formulate the CoM information as a constant physical feature of the object, which can be applied in object discrimination or identification tasks.

II. SYSTEM DESCRIPTION

The robotic system (see Fig. 1) is composed of a 6-DoF UR10 (Universal Robots) robotic arm, a RoboIQ 3-finger industrial gripper, and an OptoForce sensor set.

The gripper has three fingers, denoted as A, B, and C. The OptoForce OMD-20-SE-40N 3D tactile sensor set has four sensor nodes, each one can measure 3D forces on its surface. A corresponding *Sensor Coordinate Frame* (SCF) is defined for each sensor node on the vertex of its external semi-sphere surface¹ (see Fig. 1). Three sensor nodes were installed on each fingertip of the gripper. The sensing point of each finger (i.e. fingertip installed with tactile sensor node) are denoted as P_A , P_B , and P_C , respectively; P_B and P_C are on the same side and symmetric with respect to P_A . The *World Coordinate Frame* (WCF) is a Cartesian coordinate system located at the origin of the workspace. The table surface is set as the *reference plane*. The workspace is a cuboid volume above the reference plane: $[\underline{x}_W, \bar{x}_W] \times [\underline{y}_W, \bar{y}_W] \times [\underline{z}_W, \bar{z}_W]$, and spacial position located inside is denoted as (x_W, y_W, z_W) .

We use *normal force* f_i^n to denote the amplitude of the force component in Z_S^+ direction, which is also referred to as the *grasping force*. The tangential force can be decomposed into two components: the one along Z_S^+ axis is named *lifting force*, and denoted as f_i^l , while the other component is neglected, since it does not influence the analysis.

III. METHODOLOGY

We first introduce the estimation of geometric information of target objects in Sec. III-A; the tactile-based criterion for CoM and the CoM exploration strategy are analyzed from Sec. III-B to Sec. III-C, followed by the extraction of CoM feature in Sec. III-D.

A. Tactile-based Object Geometric Information Estimation

We explain how to continuously explore the shape of a quadrilaterally-faced hexahedron object in order to estimate its geometric information, which is required for the CoM exploration.

Tactile information detected on the sensor node is used as feedback to control the movement of the robot. Two kinds of points are of interest during exploration: *contact point*, which is detected when the exploratory sensor touches the object surface, i.e. as soon as the resultant force measured on the exploratory sensor has exceeded a pre-determined small value ($|\mathbf{f}_A| > \bar{f}_\epsilon$); and *separate point*, which is detected when the exploratory sensor detaches from the contacted object, i.e. as soon as the temporal resultant force detected by the exploratory sensor reduces below a threshold ($|\mathbf{f}_A| < \underline{f}_\epsilon$).

The proposed approach can be applied to quadrilaterally-faced hexahedron objects, whose faces are quadrilaterals. Each face can be defined by detecting three non-collinear contact points on it. Then explore the contacted face by moving from contact points on the plane towards different directions, the robot can collect separate points on edges of

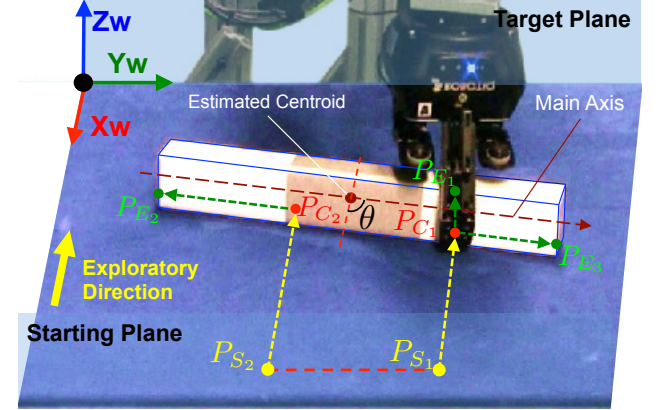


Fig. 2: The continuous exploration of a cuboidal experimental object in an unknown workspace.

the face, whereas each edge is determined by two separate points. As soon as all of the edges are known, the vertices of this side face are obtained; and the geometric information, such as location, orientation, and shape, can be estimated based on all the vertices of this target object.

Here we take a cuboidal object as example (see Fig. 2), and explain the continuous exploration process in detail. To increase the available exploration space, only one finger is stretched out, which is referred to as the *exploratory finger*, while the other two fingers are curled up. The sensor node installed on the fingertip of exploratory finger is referred to as the *exploratory sensor*. Without loss of generality, defined the X_W^- axis as the exploratory direction, and the plane perpendicular to it, i.e. \bar{X}_W - Y_W - Z_W , as the starting plane (all points on this plane satisfy $x = \underline{x}_W$), while X_W - Y_W - Z_W as the target plane ($x = \bar{x}_W$). The gripper first stretches out the exploratory finger (e.g. finger A), moves the exploratory sensor to a *starting position* P_{S_1} on the starting plane, and adjusts the orientation of the exploratory sensor towards X_W^- direction. Then the robot pushes the exploratory sensor towards the exploratory direction and tries to detect contact with the target object. If a contact point is detected, the current WCF coordinate of the exploratory sensor is recorded as the first contact point P_{C_1} , and the robot immediately stops its current movement. However, if no contact point is detected until the sensor node has moved to the target plane, the robot will retreat back, select another starting position, and repeat this exploration, until a contact point is detected. Since side faces of a cuboid are perpendicular to the reference plane, under this condition, only two contact points on the same side face are sufficient for representing this plane. Starting from P_{C_1} , the robot finger continues to slide² the exploratory sensor node upwards until a separate point P_{E_1} is detected, indicating the detection of an edge of object. Then, the robot retreats the exploratory sensor back to the starting position P_{S_1} . The robot then chooses another starting

¹The subscript “S”, “W”, and “O” denote the SCF, WCF, and OCF (object coordinate frame) coordinate frame, respectively; “+” and “-” denotes the positive and negative direction of the corresponding axis.

²Slide means that the exploratory sensor node is pressed to maintain a non-zero contact force on the face of the target object during the entire movement.

position P_{S_2} , which is selected by horizontally moving a distance from P_{S_1} on the starting plane. Starting from P_{S_2} , the robot repeats the same movement towards the X_W^- direction and tries to detect another contact point P_{C_2} . Set the line $\overleftrightarrow{P_{C_1}P_{C_2}}$ as the trajectory of the exploratory sensor, the robot slides the exploratory sensor node starting from P_{C_1} and P_{C_2} to obtain another two separate points P_{E_2} and P_{E_3} on two vertical edges of this side face. Using these collected points (two contact points to determine the plane, and three separate points to determine three edges respectively), this side face can be fully reconstructed, and all of its four vertices are obtained. After this, the robot moves to the other side of the workspace and starts exploration in the X_W^+ direction to obtain the four vertices of the opposite side face, following the same process as described above. The entire process of geometric information estimation is completed as soon as all of the vertices are obtained. Represent the set of vertices as $\{V_i\}$, $i \in 1, 2, \dots, N$ ($N = 8$ for hexahedrons), and the coordinate of V_i is (V_i^x, V_i^y, V_i^z) . The centroid of the object \mathcal{O} is calculated as $\mathcal{O} = (x_o, y_o, z_o) = \frac{1}{N}(\sum_i V_i^x, \sum_i V_i^y, \sum_i V_i^z)$, $i = 1, 2, \dots, N$. Since the object lies on the reference plane $X_W^-O_W-Y_W$, its location in the workspace is the projection of its centroid on this plane, i.e. (x_o, y_o) . We define the *main axis* l^* of the target object as the line that passes through its centroid and is parallel to the reference plane, and along which the object has the largest length. The *orientation* of the object is represented as the included angle θ , $\theta \in [-\pi/2, \pi/2]$, between its main axis and the X_W^+ axis.

The robot rotates the gripper according to θ , such that the line passes through two sensing points (P_B and P_C) is parallel to l^* . For cuboid, its length, width, and height can be easily obtained by directly calculating the distances between adjacent vertices. The origin of its OCF can locate at one arbitrary vertex, and the axes X_O , Y_O , and Z_O are defined along its length edge, width edge, and height edge, respectively.

B. Center of Mass Determination

We propose to determine the CoM of the target rigid object by applying lifting action. Consider the process of lifting a steelyard balance as an example. It can be lifted up and maintain balance without rotation if and only if the lifting force passes through its CoM.

Represent the CoM in OCF of the target object as $\mathcal{C} = (c_x, c_y, c_z)$. Each component can be determined by searching for one point of application for the lifting force along the corresponding axis in OCF; through this point of application, the object can be lifted up while maintaining equilibrium state. We take the determination of c_x as an example. In this work, we discuss the three-sensing-point case (each contact point can sense the force signals), satisfying that (1) two sensing points (e.g. P_B and P_C) are aligned on the one side of the grasped object, and (2) their positions are symmetric with respect to the other sensing point (e.g. P_A) on the opposite side of the object. This condition can be satisfied here by controlling the gripper in pinch mode. While applying *lifting action* to the target object, the gripper grasps the object at one

lifting position and lifts it up for a small distance Δh . At the equilibrium, both *force condition* and *torque condition* are satisfied, which state that both resultant force and resultant torque applied on the object are zero. We show that during lifting, the force condition can be checked via linear slip detection, whereas the torque condition can be verified by detecting the rotation of the target object.

1) Force Condition Verification via Linear Slip Detection:

According to the Coulomb's law of friction, the largest value of fiction that the gripper can provide is $\mu \cdot f_N$, where μ is the friction coefficient on the contact plane and is considered as a constant value. If the grasping force applied by the gripper is insufficient, the resultant lifting force $F = \sum f_i^l$ is not able to balance the gravity, and linear slip happens on the grasping point, i.e. $F < G - F_N$, G is the weight of the object and F_N is the supporting force from the table (if exists). Force condition is sufficient but not necessary for equilibrium state, it can be satisfied by regulating the grasping force. The force regulation is realized by linear slip detection on each one of the contact points. We detected linear slip signals by measuring the changing rate of tangential force on the contact surface [12].

If slip signal is detected on anyone of the contact points, the applied grasping force is considered insufficient. Then the gripper increases its grasping force by further closing its fingers and tries to lift the object again. The robot repeats this procedure until the target object can be lifted up to the target height without linear slip, indicating the satisfaction of force condition. The next step is to check the torque condition.

2) Torque Condition Verification via Rotation Detection:

Torque is hard to measure without torque sensors' feedback. Non-zero resultant torque applied on the object causes rotation of the object with respect to the contact point, hence we verify the torque condition by detecting the rotation of the target object during lifting process. Due to the positional symmetry, the tangential forces on P_B and P_C should be equal during the entire lifting process, if and only if the object is in equilibrium, i.e. tangential force applied on P_A passes through the CoM. Represent the sequence of force signals that recorded continuously on contact point i during lifting process as \mathbf{f}_i , $i \in A, B, C$. According to the analysis above, if \mathbf{f}_B is highly similar to \mathbf{f}_C , it can be concluded that the current lifting position is close to the real CoM of the object.

We propose to use the cross-correlation to measure the similarity of force signal sequences due to its robustness and sensitiveness. Cross-correlation measures the correlation between two jointly stationary series and has a normalized measurement in the range of $[-1, 1]$ (see Fig. 3). The cross-correlation criterion for checking the torque condition can be formulated as:

$$\rho_{BC} = \frac{\text{cov}(\mathbf{f}_B, \mathbf{f}_C)}{\sigma_{\mathbf{f}_B} \sigma_{\mathbf{f}_C}} \geq \delta, \quad \rho_{BC} \in [-1, 1], \quad \delta \in (0, 1) \quad (1)$$

with $\text{cov}(\mathbf{f}_B, \mathbf{f}_C)$ being the cross-covariance of \mathbf{f}_B and \mathbf{f}_C , whereas $\sigma_{\mathbf{f}_B}$ and $\sigma_{\mathbf{f}_C}$ the standard deviation of \mathbf{f}_B and \mathbf{f}_C , respectively. The closer ρ_{BC} to 1, the higher the similarity between \mathbf{f}_B and \mathbf{f}_C . This criterion is independent of the

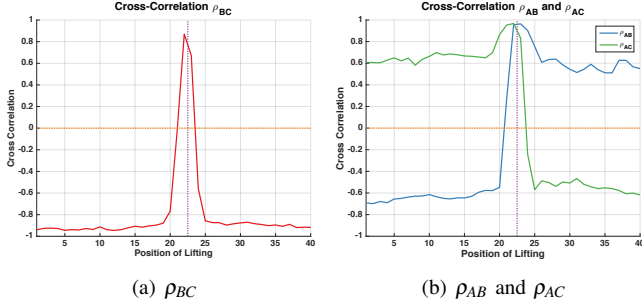


Fig. 3: The cross-correlations (Y axis) at different lifting positions (X axis) along the X_O axis of an experimental object. At each position, the robot stably lifted the object to $\Delta h = 30\text{mm}$. Lifting forces on each contact point are recorded during lifting for analysis.

absolute force values and thus can be applied on objects of different shapes, textures, and stiffness.

To determine if a lifting position can be estimated as CoM, the robot first tries to lift the object at this position and regulates its grasping force via linear slip detection. Once the force condition is satisfied, the robot evaluates ρ_{BC} for the torque condition. If ρ_{BC} is close to 1, the current lifting position is considered close to the CoM.

C. Center of Mass Exploration

Now we explain how to search for the CoM of a regular shaped rigid object along one dimension. The geometric information estimated in Sec. III-A is required. In the following, we take the exploration of c_x (in the X_O -axis) as an example. At the target lifting position, both force condition and torque condition can be satisfied. The binary search algorithm of the computational complexity $\mathcal{O}(\log_2 N)$ (for N possible sampling points) is the optimal candidate for this one-dimensional search problem, and tactile feedback is used to guide the search.

In this three-sensing-point case, we show that between the two contact points on the same side (e.g. P_B and P_C), the one that is closer to the real CoM of the target object senses larger linear friction force than the other while the object is lifted up by these three contact points.

Since the lifted object does not move horizontally, normal forces satisfy $f_1^n = f_2^n + f_3^n$; and due to the symmetry of P_B and P_C , $f_2^n = f_3^n \triangleq f^n$. Assume the object does not rotate with respect to the main axis, thus it holds that $f_1^l = f_2^l + f_3^l$ according to the torque condition. Represent the ratio of f^l to f^n for contact points 2 and 3 as α and β , respectively. Since force condition is satisfied, no linear slip happens on the contact surface:

$$f_2^l = \alpha f_2^n \leq \mu f_2^n = \mu f^n, \quad (2)$$

$$f_3^l = \beta f_3^n \leq \mu f_3^n = \mu f^n. \quad (3)$$

Forces in Z_W axis balance and meet $f_2^l + f_3^l = (mg - f_N)/2$, where f_N is the supporting force from the reference plane ($f_N = 0$ if the object is not supported by the table). Select the

reference point on the main axis, and the distances between each lifting force vector to the reference point are denoted as r_i , $i = 1, 2, 3$; r_g denotes the distance from the weight vector mg to the reference point. According to the torque condition, $r_1 f_1^l + r_2 f_2^l + r_3 f_3^l = m g r_g$ with m being the mass of the object and \mathbf{g} the gravitational acceleration.

Reformulating the above equations result in:

$$\alpha + \beta = (mg - f_N)/(2f^n) > 0, \quad (4)$$

$$(r_1 + r_2)\alpha + (r_1 + r_3)\beta = m g r_g / f^n, \quad (5)$$

and thus the following relationship holds:

$$\alpha + \beta = ((r_1 + r_2)\alpha + (r_1 + r_3)\beta)/C, \quad (6)$$

$$C = \frac{2m g r_g}{m g - f_N} > 0. \quad (7)$$

Without loss of generality, we assume $r_3 > r_2$. Since $(\alpha + \beta)f^n$ represents the minimal resultant lifting force to maintain force condition in Z_W direction, for a given f^n , $\alpha + \beta$ has the minimal possible value. If $\alpha > 0$, $\beta > 0$, according to Eq. 6, $\alpha + \beta$ reaches its minimum value if and only if $\alpha/\beta = (r_1 + r_3)/(r_1 + r_2)$. Then $\alpha > \beta$ and $f_2^l > f_3^l$. If $\alpha \cdot \beta < 0$, then $\alpha > 0 > \beta$ and $|\alpha| > |\beta|$, and $f_2^l > f_3^l$ is also satisfied. Fig. 3(b) shows an experimental verification of this conclusion. This conclusion is used to determine the next lifting position. We use the cross-correlation ρ_{AB} and ρ_{AC} to evaluate the similarity of signal sequences. The next lifting position lies in the range that is closer to the contact point that senses larger tangential force. For example, if $\rho_{AB} > \rho_{AC}$, the next lifting position should be closer to P_B while further to P_C .

In each exploration step, the robot bisects the remaining search region and chooses the middle point as the next lifting position, until has found one lifting position that can be estimated as the CoM.

D. CoM Feature Extraction

The CoM feature is defined with respect to the OCF. Along each dimension of the OCF, the edge of the object is segmented by the CoM component into two parts. We use the superscript “+” to denote the longer segment and “-” the shorter segment. Then in each dimension, the CoM feature is defined as the ratio of these two parts.

$$\boldsymbol{\lambda} = (\lambda_x, \lambda_y, \lambda_z) = (x_O^-/x_O^+, y_O^-/y_O^+, z_O^-/z_O^+). \quad (8)$$

Each component of $\boldsymbol{\lambda}$ is normalized in $(0, 1]$. As long as the OCF is determined, the CoM feature can be extracted as a constant vector.

IV. EXPERIMENTAL EVALUATION

We designed two scenarios to experimentally evaluate the performance of our proposed approaches. In the first scenario, the robot estimated target object’s geometric information and then explored its CoM. Experimental objects of distinct textures, stiffness, and sizes were used. In the second scenario, the robot tried to discriminate several experimental objects according to their CoM features.

Object 1	Object 2	Object 3	Object 4	Object 5	Object 6
S: + T: - C: +	S: ++ T: - C: +	S: + T: ++ C: +	S: ++ T: - C: +	S: ++ T: ++ C: +	S: + T: - C: ++
Object 7	Object 8	Object 9	Object 10	Object 11	Object 12
S: - T: - C: 0	S: - T: - C: ++	S: - T: - C: +	S: - T: ++ C: 0	S: - T: + C: ++	S: - T: ++ C: +

Fig. 4: Experimental objects. ‘S’: stiffness, from very soft (--) to very hard (++) . ‘T’: textural properties, ranging from very fine (--) to very rough (++) . ‘C’: distance between CoM and geometric center, ‘0’ means CoM coincides geometric center, while ‘++’ indicates CoM is far from geometric center.

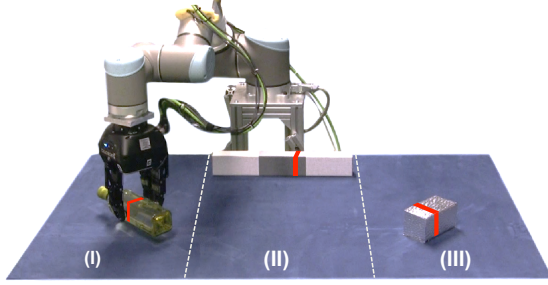


Fig. 5: For multiple objects, the entire workspace is segmented into different regions, i.e. (I), (II), and (III), and the robot explores target object located in each region.

In this work, we used cuboidal objects and only consider the 1D CoM feature λ_x (i.e. the length edge of the object), due to the hardware constraints, which mainly come from the shape of the gripper. In addition, neither location nor orientation of the target object is supposed to change after the geometric information estimation. Therefore, to maintain the stability of the target object during CoM exploration, cylinder-shaped objects or objects with curved surfaces are not taken into consideration.

A. CoM Exploration of Single Experimental Object

In this scenario, the task of the robot is to explore the CoM of several experimental objects, which have different physical properties, such as shape, textures, stiffness, and CoM locations. Due to the hardware constraint, it is difficult to estimate the geometric information of all the target objects simultaneously. For multiple target objects (see Fig. 5), the entire workspace is segmented into several regions, and the robot explores each one of the target objects located in the corresponding region successively.

Here we take the object in the region (II) as an example. Fig. 6 shows the reconstructed object after the geometric information estimation (see Fig. 2). The size of Object 1 was estimated as $40.2\text{mm} \times 3.6\text{mm} \times 5.8\text{mm}$, while the measured real size is $40.0\text{mm} \times 3.8\text{mm} \times 6.0\text{mm}$.

Then the robot adjusted the orientation of the gripper and started to explore the CoM along the X_O axis (see Fig. 8). At each lifting position, the object was lifted up to $\Delta h = 30\text{mm}$ above the reference plane. The CoM exploration terminates as soon as either the next search range is smaller than 10mm

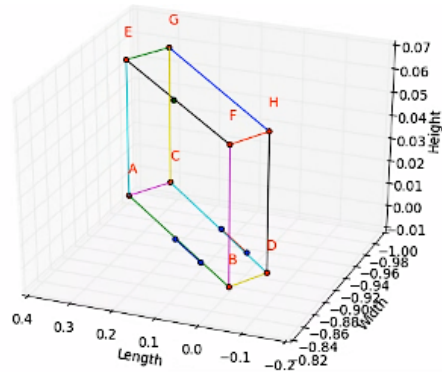


Fig. 6: The reconstructed shape of the target object.

TABLE I: Explored CoM Features of Experimental Objects

Object Nr.	1	2	3	4	5	6
λ_x	0.784	0.865	0.897	0.579	0.600	0.428
Object Nr.	7	8	9	10	11	12
λ_x	0.998	0.291	0.833	0.909	0.218	0.769

or $\rho_{BC} > \delta = 0.9$. The CoM component was estimated as $\lambda_x = 0.681$ within six steps, with an error range of $L \times 2^{-6} = 6.25\text{mm}$ ($L = 40.0\text{mm}$).

The estimated CoM components λ_x of each experimental object are listed in Table I.

Object 1	Object 2	Object 3
S: + T: -- C: 0	S: + T: -- C: +	S: + T: -- C: ++

Fig. 7: We deliberately manufactured three experimental objects, which have identical stiffness, surface textures, and sizes, while distinct CoMs (marked by the red region).

B. CoM-based Object Discrimination

Three manufactured objects (see Fig. 7) are used in this scenario (see Fig. 1). They have the identical physical properties, while their CoMs are modified to be distinct by deliberately adjusting their inner structures.

The robot collected the CoM feature of each object for 20 trials. The mean values of the explored λ_x of each experimental object are listed in Table II. This 1D dataset was clustered by segmenting the estimated kernel density at its local minimum values. We used Gaussian kernel with a bandwidth of 0.025 for the KDE (Kernel Density Estimation) analysis. Result shows that the sampled CoM featured can be clustered into three classes, with an adjusted rand index of 1.0, indicating that all the collected CoM features are successfully clustered (see Fig. 9).

TABLE II: Explored CoM Features in Sec. IV-B

Object Nr.	1	2	3
λ_x	0.927	0.784	0.346

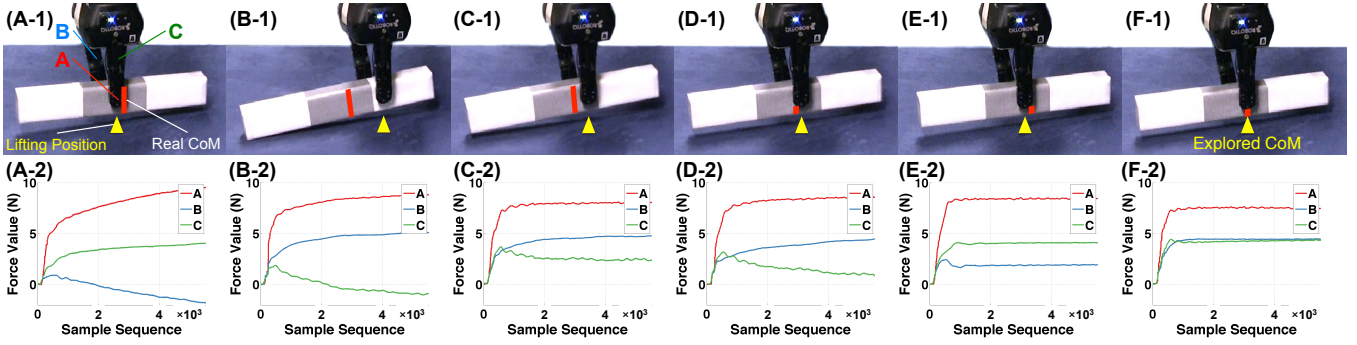


Fig. 8: The process of exploring the CoM of a regular shaped rigid object using binary search approach based on tactile feedback. In each column, the upper subfigures (A-1) - (F-1) show the lifting position at each sample step. The real CoM of this target object is marked by the red region, and the yellow triangle in each figure indicates the current lifting position. The lower subfigures (A-2) - (F-2) show the corresponding sensor signal sequences of each finger recorded during lifting.

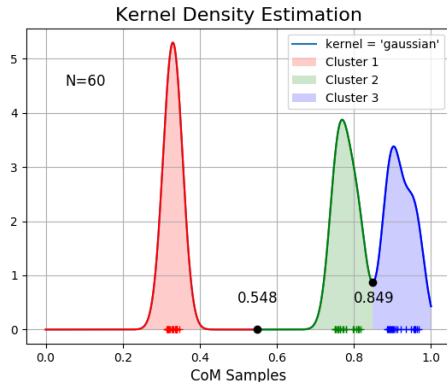


Fig. 9: Clustering result of CoM features based on KDE.

V. CONCLUSION AND FUTURE WORK

In this paper, we proposed a tactile-based approach to explore the CoM of rigid objects in an unknown workspace for robotic object discrimination tasks. We first presented a continuous exploration approach for the robot to estimate target object's geometric information, which can be applied to quadrilaterally-faced hexahedron objects. Then, we analyzed the conditions that the applied force and torque should satisfy when the object is lifted up at its CoM, and proposed the strategy to explore the CoM of a target rigid object. It is worth mentioning that the applicability of the proposed CoM exploration approach is independent of the number of grasping fingers, rather only depends on the sensing points. Furthermore, we formulated the CoM information as a constant feature defined in the OCF, which is insusceptible to the external properties of the object and can be applied in object discrimination and recognition tasks.

The scope of this work is focused on the regular shaped rigid objects. In the future, we plan to generalize our approach for irregular shaped objects or soft objects by removing the constraints from hardware, i.e. using dexterous robotic hand and multi-modal tactile sensors. In our proposed method, at least three sensing points are required to detect the rotation of lifted object. The number of sensing points can be further reduced if the occurrence and direction of

rotational slip can be detected. In addition, it is possible to accelerate the exploration process of the CoM for a novel object by taking advantage of the prior knowledge, i.e. by transferring the mass distribution information of the explored objects to a novel target object.

ACKNOWLEDGMENT

Many thanks to OptoForce Ltd. for providing tactile sensors for this study.

REFERENCES

- [1] R. S. Dahiya, G. Metta, M. Valle, and G. Sandini, "Tactile sensing—from humans to humanoids," *IEEE Transaction on Robotic*, vol. 26, no. 1, pp. 1–20, 2010.
- [2] M. Kaboli, P. Mittendorfer, V. Hugel, and G. Cheng, "Humanoids learn object properties from robust tactile feature descriptors via multimodal artificial skin," *IEEE Int. Conf. on Humanoid Robots*, 2014.
- [3] M. Kaboli, R. Walker, and G. Cheng, "In-hand object recognition via texture properties with robotic hands, artificial skin, and novel tactile descriptors," *IEEE International Conference on Humanoid Robots*, pp. 2242–2247, 2015.
- [4] M. Kaboli, R. Walker, and G. Cheng, "Re-using prior tactile experience by robotic hands to discriminate in-hand objects via texture properties," *IEEE International Conference on Robotics and Automation*, pp. 2242–2247, 2016.
- [5] M. Kaboli, D. Feng, K. Yao, P. Lanillos, and G. Cheng, "A tactile-based framework for active object learning and discrimination using multimodal robotic skin," *IEEE Robotics and Automation Letters*, vol. 2, no. 4, pp. 2143–2150, 2017.
- [6] M. Kaboli, D. Feng, and G. Cheng, "Active tactile transfer learning for object discrimination in an unstructured environment using multimodal robotic skin," *International Journal of Humanoid Robotics*, 2017.
- [7] C. G. Atkeson, C. H. An, and J. M. Hollerbach, "Rigid body load identification for manipulators," *IEEE Conference on Decision and Control*, pp. 996–1002, 1985.
- [8] C. H. An, C. G. Atkeson, and J. M. Hollerbach, "Estimation of inertial parameters of rigid body links of manipulators," in *IEEE Conference on Decision and Control*, vol. 24, pp. 990–995, 1985.
- [9] Y. Yu, K. Fukuda, and S. Tsujio, "Estimation of mass and center of mass of graspless and shape-unknown object," in *IEEE International Conference on Robotics and Automation*, vol. 4, pp. 2893–2898, 1999.
- [10] Y. Yu, T. Kiyokawa, and S. Tsujio, "Estimation of mass and center of mass of unknown and graspless cylinder-like object," *International Journal of Information Acquisition*, vol. 1, no. 01, pp. 47–55, 2004.
- [11] Y. Yu, T. Arima, and S. Tsujio, "Estimation of object inertia parameters on robot pushing operation," in *IEEE International Conference on Robotics and Automation*, pp. 1657–1662, 2005.
- [12] M. Kaboli, K. Yao, and G. Cheng, "Tactile-based manipulation of deformable objects with dynamic center of mass," *IEEE International Conference on Humanoid Robots*, pp. 790–799, 2016.